MATEC Web of Conferences **21**, 12008 (2015)
DOI: 10.1051/matecconf/20152112008

Constitutive modelling of creep-ageing behaviour of peak-aged aluminium alloy 7050

Yo-Lun Yang[1,a], Aaron C.L. Lam[1], Zhusheng Shi[1], Jianguo Lin[1], and Rajab Said[2]

[1] Department of Mechanical Engineering, Imperial College London, London SW7 2AZ, UK
[2] ESI Group, 100-102, Avenue de Suffren, Paris 75015, France

Abstract. The creep-ageing behaviour of a peak-aged aluminium alloy 7050 was investigated under different stress levels at 174 °C for up to 8 h. Interrupted creep tests and tensile tests were performed to investigate the influences of creep-ageing time and applied stress on yield strength. The mechanical testing results indicate that the material exhibits an over-ageing behaviour which increases with the applied stress level during creep-ageing. As creep-ageing time approaches 8 h, the material's yield strength under different stress levels gradually converge, which suggests that the difference in mechanical properties under different stress conditions can be minimised. This feature can be advantageous in creep-age forming to the formed components such that uniformed mechanical properties across part area can be achieved. A set of constitutive equations was calibrated using the mechanical test results and the alloy-specific material constants were obtained. A good agreement is observed between the experimental and calibrated results.

1. Introduction

Creep-age forming (CAF) is a state-of-the-art metal processing method that combines age hardening and inelastic deformation. Conventional forming process involving several heat treatments and forming processes could be merged into the CAF process to greatly reduce the cost. CAF plays a pivotal role in manufacturing lightweight and large pieces, such as the wing panels of airplanes and aluminium panels used in aerospace applications. The deformation process in CAF is primarily based on the creep phenomenon deliberately induced during the age/precipitation hardening process [1].

7000-series aluminium alloys are widely applied in the aerospace industries due to its good strength-to-weight ratio [2]. The strength of these alloys are generally attributed to the fine and uniformly dispersed precipitates formed during the artificial ageing process [3]. The precipitation transformation sequence can be described as [4]:

$$\text{Solid solution}(\alpha) \rightarrow \text{GP zones} \rightarrow \eta' - \text{MgZn}_2 \rightarrow \eta\text{-MgZn}_2.$$

The η' precipitate is the main phase in peak-aged condition (T7 temper) [5]. At this stage, fatigue and stress corrosion cracking (SCC) resistances of the alloy are very low. The SCC resistance is mainly

[a] Corresponding author: Y.Yang13@Imperial.ac.uk

Table 1. Chemical composition of AA7050-T7 (wt%).

Al	Zn	Mg	Cu	Fe	Si	other
Bal.	6.247	2.143	2.231	0.049	0.033	0.150

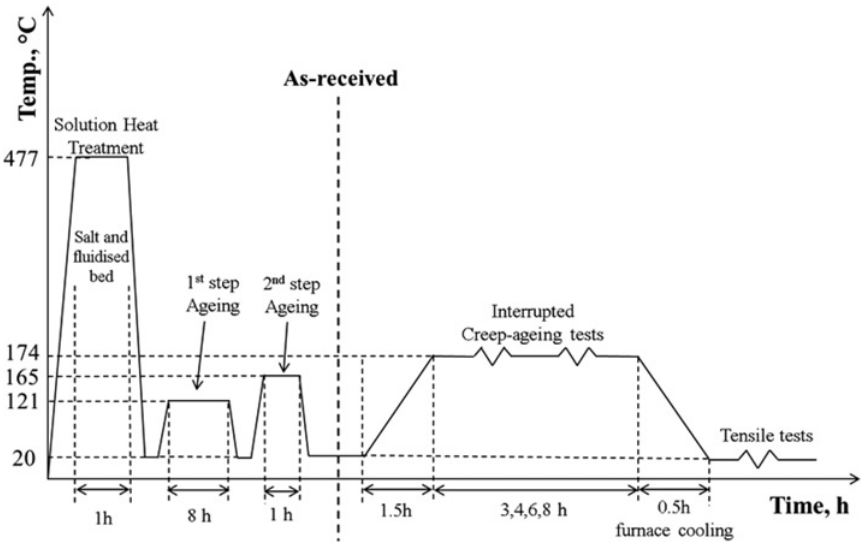

Figure 1. Heat treatment process of the as-received material and test procedure.

influenced by grain boundary precipitates [6]. To satisfy the requirement of enhanced SCC resistance for aerospace applications, over-ageing (T8 temper) treatment is normally introduced to transform the η' precipitate to the η precipitate. This treatment can increase the precipitate size and inter-particle distance between grain boundary precipitates [7]. Under the over-ageing treatment, the material's strength usually decreases by 10 to 15% from peak-aged to over-aged condition [8, 9].

Many constitutive models for CAF have been developed to predict the mechanical properties and form shape so that a specific strength and part shape can be achieved [10, 11]. Zhan et al. [12] proposed a set of mechanism-based unified creep-aging constitutive equations to model creep deformation and the evolutions of precipitate size and dislocation density, which control the amount of age hardening, solid solution hardening and work hardening during creep-ageing. The model was applied to the creep-ageing treatment of AA7055 from the as-quenched or T3 to T4 conditions. However, work on contitutive modelling with respect to creep-ageing properties in the over-aged condition is limited.

The purpose of this research is to investigate both the over-ageing and creep behaviour of AA7050-T7 via mechanical testing. A set of creep-ageing constitutive equations is presented and calibrated using the test data. These constitutive equations can be used to predict the creep properties and yield strength of AA7050-T7.

2. Experimental details

2.1 Material

The material used in this study was AA7050-T7 whose chemical composition is listed in Table 1. The heat treatment process is illustrated in Fig. 1. The material was first solution heat treated at 477°C for 1 h. It was then subjected to first-step-ageing at 121°C for 8 h and a second-step-ageing at 165°C for 1 h.

Table 2. Initial values of the material model.

σ_A (MPa)	σ_{ss} (MPa)	σ_{dis} (MPa)	$\bar{\rho}$	$\bar{r}$
300.0	273.4	0.0	0.0	1.0

2.2 Experimental procedure

Test specimens were machined from the as-received temper state. Two steps of mechanical testing were carried out as shown in Fig. 1. The first step is uniaxial creep-ageing test under different stress levels and ageing times at a constant ageing temperature and the second step is room temperature tensile test of the creep-aged specimens, which was carried out to determine the creep-age hardening properties of the material.

Creep-ageing tests were conducted in air with different initial stresses from 0 MPa (pure ageing) to 175 MPa, in the intermediate temperature range of 174°C for 3–8 h. The creep specimens had a diameter of 8 mm and a gauge length of 36 mm, which complies with the ASTM E8 standard. The creep strain was measured using two linear capacitance gauges fitted on the ridges of the samples to measure the displacement. After creep-ageing, tensile tests were performed at a strain rate of $10^{-4}\,s^{-1}$ under room temperature for the yield strength evolution to be determined.

3. Constitutive modelling

3.1 Constitutive equations

The constitutive equations proposed by Zhan et al. [12] were selected and are presented as Eqs. (1)–(7). Equation (1) describes the creep strain evolution. Creep strain rate ($\dot{\varepsilon}_c$) is a function of applied stress during creep (σ), normalised dislocation density ($\bar{\rho}$) and the material's yield strength (σ_y). σ_y is determined by age hardening (σ_A), solid solute hardening (σ_{ss}) and dislocation hardening (σ_{dis}), which are presented in Eqs. (2)–(5). These hardening effects are influenced by the normalised precipitate size ($\bar{r}$) and $\bar{\rho}$ whose rate equations are shown in Eqs. (6) and (7). The $\bar{r}$ is defined as $\bar{r} = r/r_c$ where r_c is the precipitate size at peak-aged condition. The $\bar{\rho}$ is defined as $\bar{\rho} = (\rho - \rho_i)/\rho_m$ where ρ_i is the dislocation density at the initial state before ageing and ρ_m is the saturated dislocation density. The growth rate of normalised precipitate size ($\dot{\bar{r}}$) is related to the dislocation density ($\bar{\rho}$).

These equations are able to model the creep-age hardening behaviour of aluminium alloys from the as-quenched or T3 to T4 conditions. In order to model the over-ageing behaviour of the present alloy, initial parameters of the material need to be modified. Table 2 shows the chosen initial values.

$$\dot{\varepsilon}_c = A_1 \sinh\{B_1[|\sigma|(1-\bar{\rho}) - k_0\sigma_y]\}\text{sign}\{\sigma\} \tag{1}$$

$$\sigma_y = \sigma_{ss} + \sqrt{\sigma_A^2 + \sigma_{dis}^2} \tag{2}$$

$$\dot{\sigma}_A = C_A \dot{\bar{r}}^{m_1}(1-\bar{r}) \tag{3}$$

$$\dot{\sigma}_{ss} = C_{ss} \dot{\bar{r}}^{m_2}(\bar{r}-1) \tag{4}$$

$$\dot{\sigma}_{dts} = A_2 \cdot n \cdot \bar{\rho}^{n-1}\dot{\bar{\rho}} \tag{5}$$

$$\dot{\bar{r}} = C_r\,(Q-\bar{r})^{m_3}\left(1+\gamma_0\bar{\rho}^{m_4}\right) \tag{6}$$

$$\dot{\bar{\rho}} = A_3(1-\bar{\rho})|\dot{\varepsilon}_c| - C_p\bar{\rho}^{m_5}. \tag{7}$$

Table 3. Constants of the CAF constitutive equations for AA7050-T7 at 174 °C.

A_1 (h^{-1})	B_1 (MPa^{-1})	k_0	C_A (MPa)	m_1	C_{ss} (MPa)	m_2	n	A_2 (MPa)
2.082E-5	0.04	0.097	25	0.5	-1.6	0.806	1.425	90
C_r (h^{-1})	Q	γ_0	m_3	m_4	A_3	C_p (h^{-1})	m_5	
0.3	3	50	0.75	3.3	220	0	0	

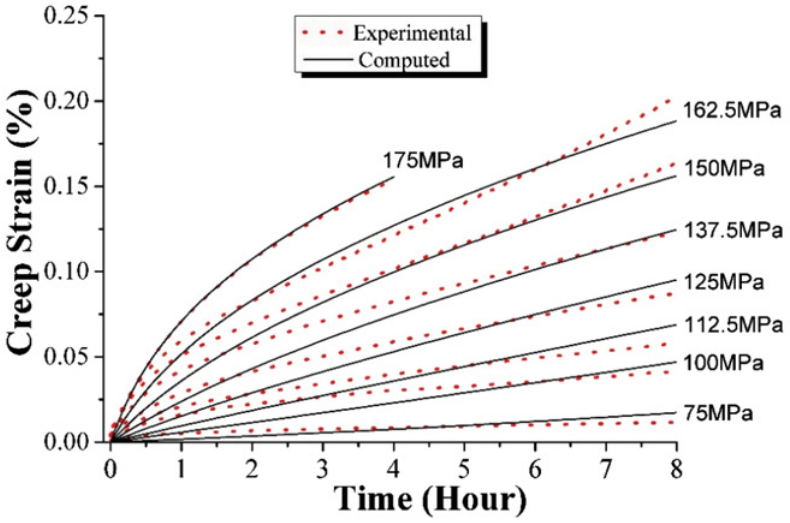

Figure 2. Experimental (dashed lines) and computed (solid lines) creep-ageing curves for different stress levels at 174°C.

3.2 Determination of material constants

The material constants of the constitutive equations were determined by fitting the experimental creep curves and yield strengths evolutions. The fitting process can be divided into three stages:

- Stage 1: Determination of the material constants relating to normalised precipitate size and dislocation density using experimental results on yield strength evolution with time under pure ageing (0 MPa) and creep-ageing conditions.

- Stage 2: Determination of material constants relating to yield stress using experimental results on yield strength evolution with time under different stress levels.

- Stage 3: Re-evaluation of all predetermined material parameters according to the experimental creep data and yield strength data, and optimisation of them in Stage 1-2 to obtain the best-fit results.

4. Result and discussion

The material constants for the constitutive equations determined following the above procedure are listed in Table 3. Figures 2 and 3 show comparisons of the experimental and computed results. A steady state creep stage is observed in this alloy under the applied stress of up to 162.5 MPa. Under 175 MPa, tertiary creep occurred after 4 h of creep-ageing. The creep curve fitting show good agreements at all stress levels. Under 175 MPa, however, the fitting can only be used to predict creep-ageing behaviour up to 4 h because of the occurrance of tertiary creep after that, to which the current model is not applicable.

Tensile tests after creep-ageing for different length of time indicate a decrease in the material's strength, as shown in Fig. 3. The effect of applied stress during creep and creep-ageing time on the yield strength can be observed. An increase in the applied stress during creep-ageing accelerates the

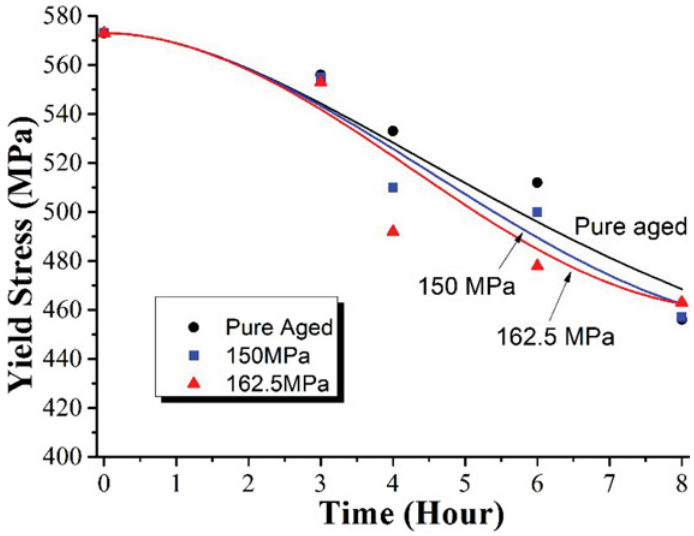

Figure 3. Experimental (symbols) and computed (solid lines) yield stress evolution under different stress levels at 174°C.

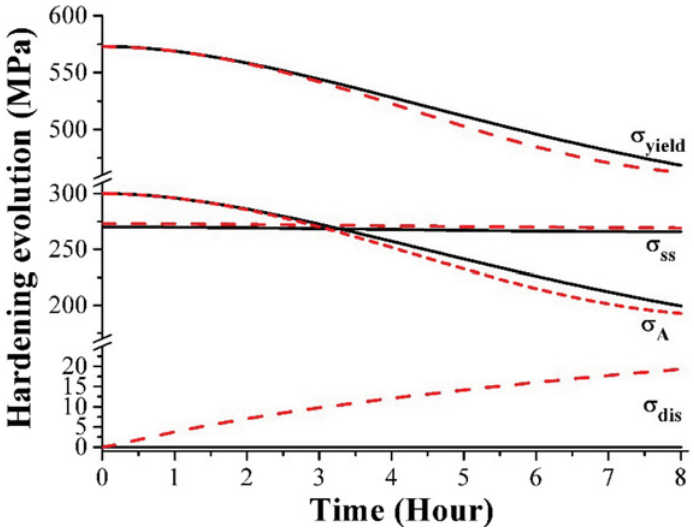

Figure 4. Computed creep-age hardening yield strength at 0 MPa (solid curve) and 162.5 MPa (dashed curve).

decreasing rate of the yield strength, which is a typical over-ageing behaviour. As the creep-ageing time increases further, the material's strengths under different stress levels gradually converge.

A detailed prediction for the contributions of yield strength (σ_y) from solid solution hardening (σ_{ss}), dislocation hardening (σ_{dis}) and age hardening (σ_A) are shown in Fig. 4. It can be seen that σ_{dis} is relatively small in comparison with σ_{ss} and σ_A. σ_{ss} decreases slightly with time because the solid solution has reached the steady state. σ_A is influenced by the over-ageing effect which dominates the evolution of the material's yield strength.

5. Conclusion

The present study provides a better understanding of the over-ageing properties of AA7050-T7. A set of constitutive equations was calibrated for the alloy-specific material constants to be generated. A good agreement is observed between the experimental and calibrated results. The experimental work and constitutive modelling lead to the following conclusions:

- The difference in mechanical properties of AA7050-T7 under different applied stress conditions is minimised after 8 h. This feature was captured by the model developed in this work.
- In this constitutive model the yield strength of the material takes contributions from solid solution hardening, dislocation hardening and age hardening. For this over-aged alloy, less age hardening contribution is the main factor that leads to the reduction in material's yield strength.
- The combination of the experimental work and constitutive modelling in this study contributes to better understanding of the alloy's strengthening mechanisms during the CAF process.

The authors gratefully acknowledge the support from the ESI Group, France, for the provision of research funding, test materials and specimens.

References

[1] L. Zhan, J. Lin, T.A. Dean, Int. J. Mach. Tool. Manu., **51**, 1 (2011)
[2] J.E. Hatch, *Aluminum - Properties And Physical Metallurgy*, Automot. Eng., **92**, 109 (1984)
[3] G. Sha, A. Cerezo, Acta Mater., **52**, 4503 (2004)
[4] D.J. Lloyd, M.C. Chaturvedi, J. Mater. Sci., **17**, 1819 (1982)
[5] N.Q. Chinh, J. Lendvai, D.H. Ping, K. Hono, J. Alloys Compd., **378**, 52 (2004)
[6] M. Puiggali, A. Zielinski, J.M. Olive, E. Renauld, D. Desjardins, M. Cid, Corros. Sci., **40**, 805 (1998)
[7] J.-C. Lin, H.-L. Liao, W.-D. Jehng, C.-H. Chang, S.-L. Lee, Corros. Sci., **48**, 3139 (2006)
[8] A.F. Oliveira Jr, M.C. de Barros, K.R. Cardoso, D.N. Travessa, Mat. Sci. Eng. A, **379**, 321 (2004)
[9] M. Dixit, R.S. Mishra, K.K. Sankaran, Mat. Sci. Eng. A, **478**, 163 (2008)
[10] K.C. Ho, J. Lin, T.A. Dean, Int. J. Plast., **20**, 733 (2004)
[11] K.C. Ho, J. Lin, T.A. Dean, J. Mater. Process. Technol., **153-154**, 122 (2004)
[12] L. Zhan, J. Lin, T.A. Dean, M. Huang, Int. J. Mech. Sci., **53**, 595 (2011)